17th International Conference
ENGINEERING MECHANICS 2011
Svratka, Czech Republic, 9 – 12 May 2011

PORE SIZE DISTRIBUTION OF HUMAN TRABECULAR BONE – COMPARISON OF INTRUSION MEASUREMENTS WITH IMAGE ANALYSIS

T. Doktor[*], J. Valach[*], D. Kytýř[*], O. Jiroušek[**]

Abstract: *This paper deals with pore size distribution assessment in trabecular structure of human proximal femur. Two different approaches for estimation of histograms of pore size distribution are tested, mercury intrusion porosimetry and image analysis. For the image analysis two-dimensional images of cross-sections of the specimens were used and the pore size distribution was estimated using a stereological calculation method based on the geometrical properties of an idealized pore. Comparison of the results of both methods is presented. Suitability of both methods for biological materials is discussed regarding to mechanical properties of these materials, characteristics of pores and range of pore sizes present in the structure.*

Keywords: ***Pore size distribution, image analysis, trabecular bone, mercury intrusion porosimetry.***

1. Introduction

Description of heterogeneous materials using a representative volume element is a way to simplify the analysis of their mechanical behaviour. Information about the inner structure required for the development of the representative volume element of the trabecular bone can be obtained in the form of histogram of pore size distribution. Measurements of pore size distribution in the trabecular structure of human proximal femur are described in the paper.

2. Materials and methods

2.1. Specimens

Two sets of specimens were used for the tests, both harvested from human proximal femur (male donor, 72 years old). The first set, three cylindrical specimens (diameter 5mm, height 10mm), was used for MIP measurements (Washburn, 1921). The specimens were dried using a hot air dryer at temperature 40° C for 15 hours. The second set, three slices of dimensions 20x30mm and thickness 2.5mm, was used for pore size distribution assessment using image analysis. The slices were cut using a precise saw Buehler Isomet 1000 (Buehler, Ltd., Düsseldorf, Germany) and the cylinders were prepared using a diamond hollow drill bit (Narex, s.r.o., Česká Lípa, Czech rep.). The specimens were delipidated using an ultrasonic cleaner Polsonic SONIC 3 (Polsonic Palczyński Sp. J., Warsaw, Poland) and a detergent solution Alconox (Alconox, Inc., White Plains, USA).

2.2. Mercury intrusion porosimetry

MIP measurements were performed using PoreMaster 60 GT device (Quantachrome Instruments, Inc, Boynton Beach, USA). Pressure of mercury up to $413.6 \cdot 10^6$ Pa was used, mercury surface tension was $0.48 \mathrm{N \cdot m^{-1}}$ and mercury contact angle was 140°.

[*] Bc. Tomáš Doktor, Ing. Jaroslav Valach, Ph.D. and Ing. Daniel Kytýř : Department of Mechanics and Materials, Czech Technical University in Prague, Faculty of Transportation Sciences, Na Florenci 25; 110 00, Prague; CZ, e-mails: {xdoktor, valach, xkytyr}@fd.cvut.cz

[**] Doc. Ing. Ondřej Jiroušek, Ph.D.: Institute of Theoretical and Applied Mechanics, Academy of Sciences of the Czech Republic, Prosecká 76, 190 00; Prague; CZ, e-mail:jirousek@itam.cas.cz

2.3. Image analysis

Images of the slices were acquired using a high resolution flatbed scanner EPSON Perfection V350 (Seiko Epson Corporation, Owa, Japan). Resolution 4800dpi was used (1px corresponds to 5μm). The process of identification of cross-section of pores was performed in three main steps: segmentation of the captured image, calculation of the cross-section areas and estimation of the pore size distribution. All these procedures were implemented in the Matlab computational environment (Mathworks, Inc., Natick, USA) based on functions described in Gonzales (2004). First, the images were segmented using thresholding to convert the gray-scale image into a binary form and using a concatenation of morphological operations (dilatation and erosion) to separate cross-sections of the connected pores.

In the second step, sizes of all cross-sections of the pores present in the captured image were calculated using a two-pass algorithm for connected component analysis (Shapiro & Stockman, 2001). In the third step, obtained frequencies of differently sized cross-sections of pores were converted into the histogram of pore sizes using a stereological calculation method described in (Xu & Pitot, 2003). The method is based on the geometric properties of a sphere and on the probability of affiliation of the cross-section to differently sized spheres (depicted in Fig. 1).

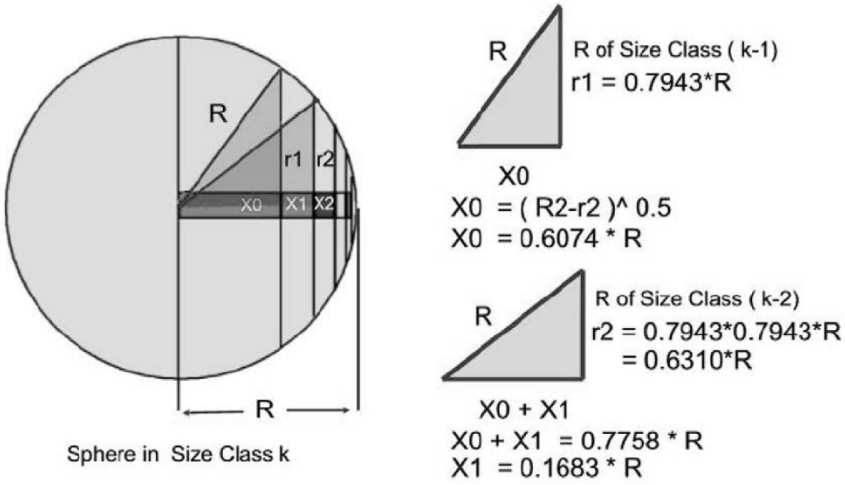

Fig. 1: Principle of the stereologic calculation (Xu & Pitot, 2003).

3. Results

Results of MIP measurements are depicted in Fig. 2. For comparison of the results of MIP with the image analysis the histogram obtained by MIP was converted into 25 size classes corresponding with the arrangement of the results of the image analysis (depicted in Fig. 3). Pore size distribution obtained by the image analysis is depicted in Fig. 4. Porosity ratios obtained by both methods are listed in Tab. 1.

Tab. 1: Comparison of volume porosity ratio obtained by MIP and by the image analysis.

Mercury intrusion porosimetry		***Image analysis***	
Sample No.	***Porosity [%]***	***Sample No.***	***Porosity [%]***
1	***69.8***	***4***	***62.8***
2	***68.7***	***5***	***59.3***
3	***45.3***	***6***	***61.7***

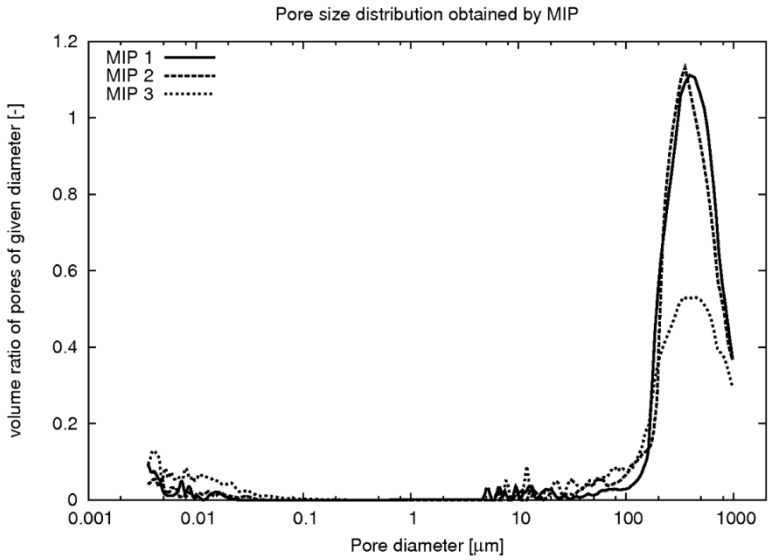

Fig. 2: Results of MIP measurements.

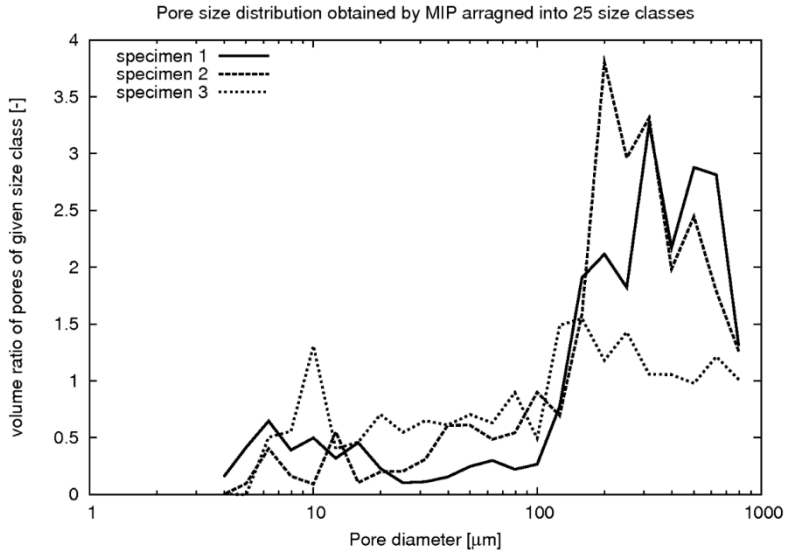

Fig. 3: Results of MIP measurements arranged into 25 size classes for a better comparison with the image analysis.

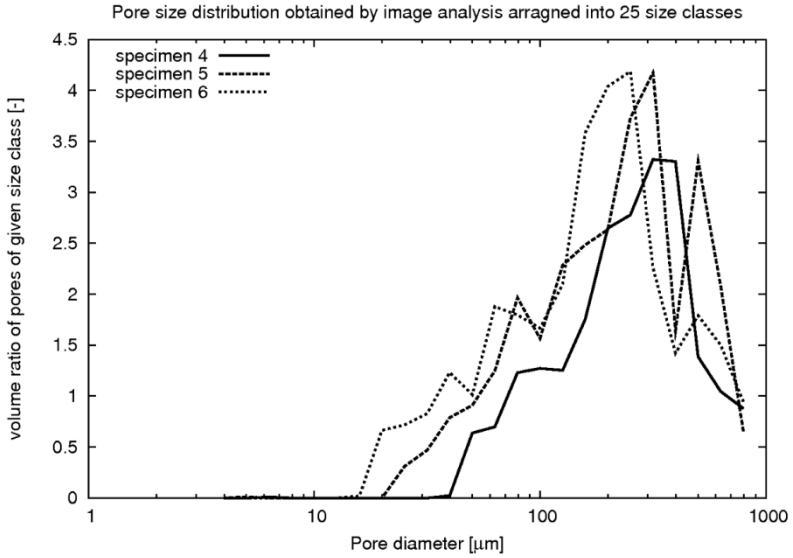

Fig. 4: Results of image analysis.

4. Discussion

By MIP two main types of porosity distinguished by Cowin (2001) were detected. The pore size up to 0.1 μm is associated with spaces between mineral crystallites and collagen. Voids detected in range from 5 μm to $9.50 \cdot 10^3$ μm belong to intertrabecular porosity.

Lower porosity ratio and lower frequency of pores of large size in case of the specimen No. 3 was caused by the previous use of this specimen in a loading test. The test had required to equip the specimen with epoxy resin reinforcement on the top and bottom bases. Therefore a part of the voids were filled by the resin and were not able to be filled by mercury.

Differences between porosity ratios obtained by MIP and image analysis are caused by the lower limit of the pore size registered by the image analysis (pores smaller than 20μm were omitted).

MIP provides histograms of pore-sizes in range from $3.50 \cdot 10^{-3}$ μm to $9.50 \cdot 10^3$ μm. The range of the pore sizes registered using the image analysis is limited by the resolution and the dimensions of the captured images and by the used stereological calculation method. The method used in this work allows to register pores in 25 size classes with the ratio between the smallest and largest size-class equal to 250 (determined by the scale factor between size classes).

Suitability of MIP for biological tissues is limited due to high mercury pressure applied by the measurement and due to the requirements for the specimens – sample volume up to 6.6 cm^3 and low humidity. The limited dimensions of the specimens make the measurements impossible for materials with high frequency of large voids. For some biologic materials (e. g. fungi) the intrusion measurements are impossible because of the requirement on the low specimen humidity or due to the high pressure applied during the intrusion measurement (both can cause undesirable changes of the inner structure).

5. Conclusions

In this study pore size distribution in trabecular structure of human proximal femur was estimated using MIP and using image analysis. Both methods show in a good agreement the largest frequency of pore size in range from 200μm to 300μm. Comparison of suitability of both methods for assessment of pore size distribution in biological materials was discussed. The main advantages of MIP are in a wide range of registered pore sizes and a high resolution. The image analysis provides the possibility of pore size distribution assessment also for materials with a high frequency of large voids (over 1000 μm) or with closed voids or materials with unfavorable mechanical properties.

The main limitation of the presented image analysis method is founded in the idealization of the voids by spheres. The used algorithm for connected component analysis provides also information about shape of pore cross-sections and therefore the analysis can be extended by estimation of predominant orientation of pores to allow estimation of anisotropic properties of the bone structure.

Acknowledgement

The research has been supported by Grant Agency of the Czech Technical University in Prague (grant No. SGS10/218/OHK2/2T/16), by the Grant Agency of the Czech Republic (grant No. P105/10/2305), research plan of the Academy of Sciences of the Czech Republic AV0Z20710524 and by research plan of the Ministry of Education, Youth and Sports MSM6840770043.

References

Cowin, S. C. (2001) Bone mechanics handbook, CRC Press, Florida, pp. 23(6-7).

Gonzales, R. C. (2004) Digital image processing using MATLAB, Upper Saddle River, Pearson.

Shapiro, L. & Stockman, G. (2001) Computer Vision, Prentice Hall.

Washburn, E. W. (1921) Note on a Method for Determining the Distribution of Pore Sizes in a Porous Material, Proceedings of National Academy of Sciences.

Xu, Y. H. & Pitot, H. C. (2003) An improved stereologic method for three-dimensional estimation of particle size distribution from observations in two dimensions and its application. Computer Methods and Programs in Biomedicine.